High-pressure synthesis of the layered iron oxyselenide BaFe_{2}Se_{2}O with strong magnetic anisotropy

Fumitaka Takeiri, Yuki Matsumoto, Takafumi Yamamoto, Naoaki Hayashi, Zhi Li, Takami Tohyama, Cédric Tassel, Clemens Ritter, Yasuo Narumi, Masayuki Hagiwara, and Hiroshi Kageyama

Phys. Rev. B **94**, 184426 — Published 21 November 2016

DOI: 10.1103/PhysRevB.94.184426

High pressure synthesis of layered iron oxyselenide $BaFe_2Se_2O$ with strong magnetic anisotropy

Fumitaka Takeiri[1], Yuki Matsumoto[1], Takafumi Yamamoto[1], Naoaki Hayashi[2], Zhi Li[3], Takami Tohyama[4], Cédric Tassel[1], Clemens Ritter[5], Yasuo Narumi[6] Masayuki Hagiwara[6], and Hiroshi Kageyama[1,7]*

[1] Department of Energy and Hydrocarbon Chemistry, Graduate School of Engineering, Kyoto University, Nishikyo-ku, Kyoto 615-8510, Japan

[2] Research Institute for Production Development, Sakyo-ku, Kyoto 606-0805, Japan

[3] School of Materials Science and Engineering, Hefei University of Technology, Hefei, Anhui 230009, China

[4] Department of Applied Physics, Tokyo University of Science, Katsushika, Tokyo 125-8585, Japan

[5] Institut Laue-Langevin (ILL), 71 Avenue des Martyrs, Grenoble 38000, France

[6] Center for Advanced High Magnetic Field Science, Graduate School of Science, Osaka University, 1-1 Machikaneyama, Toyonaka 560-0043, Japan

[7] CREST, Japan Science and Technology Agency (JST), Kawaguchi, Saitama 332-0012, Japan

ABSTRACT

Using high pressure reaction, we successfully synthesized $BaFe_2Se_2O$ with a uniform stack of $[Fe_2Se_2O]$ layers. Magnetic susceptibility, heat capacity, Mössbauer spectroscopy, and neutron diffraction measurements revealed that $BaFe_2Se_2O$ undergoes antiferromagnetic order at 106 K with a 2-***k*** spin structure, where each Fe moment points to a neighboring oxide anion. The same spin structure has been observed in the related iron oxyselenides, but with a staggered stack of $[Fe_2Ch_2O]$ layers (*Ch* = S, Se). We propose that the strong uniaxial anisotropy inferred from the 2-***k*** structure originates from spin-orbit coupling (SOC) induced by *trans*-FeO_2Se_4 octahedron, which provides a quasi-linear coordination environment as often found in single molecule magnet complexes. First principles calculation with inclusion of SOC supports the stabilization of the 2-***k*** spin structure, giving unquenched orbital momentum of 0.1 μ_B/Fe. The present study provides an idea of how to design magnetic lattices of uniaxial anisotropy using oxychalcogenides and more generally mixed anion compounds.

INTRODUCTION

Iron-based high-T_c superconductors are composed of iron atoms arranged in a regular square lattice, joined by tetrahedrally coordinated pnictogen (P, As) or chalcogen (S, Se, Te) atoms.[1,2] Superconductivity of these compounds is derived from hole- or electron-doping of their parent magnetic phases as in cuprates. However, as opposed to a (π, π) order in the undoped cuprates, they show various spin order patterns such as a stripe (π, 0) order[3] with different stacking sequences[4,5] and a bicollinear (π/2, π/2) order.[6,7] Recently, layered oxychalcogenides AM_2Ch_2O (A^{2+} = $(Ln_2O_2)^{2+}$ (*Ln* = lanthanides), $(Sr_2F_2)^{2+}$, $(Ba_2F_2)^{2+}$, $(Na_2)^{2+}$; *M* = Mn, Fe, Co; *Ch* = S, Se) consisting of $[M_2Ch_2O]^{2-}$ layers separated by A^{2+} units (Fig. 1a) have been intensively studied.[8–19] This system also possesses the square lattice of M^{2+} ions, but with heteroleptic MO_2Ch_4 coordination unlike the homoleptic local environment (e.g. $FeAs_4$ and $FeSe_4$) in Fe-based superconductors, offering a potential to extensively control electronic structures and resultant physical properties. In fact, they exhibit various spin structures such as (π, π) order in $(La_2O_2)Mn_2Se_2O$ and (π/2, π/2) order in $(La_2O_2)Co_2Se_2O$.[14,18] Particularly interesting is the case for *M* = Fe having a novel non-collinear pattern with neighboring iron moments being aligned orthogonally.[19–22] This spin structure described by double $\boldsymbol{k}$ vectors, (π/2, 0, π/2) and (0, π/2, π/2), has been predicted for a system with the tetradedral FeAs layer,[23] but without experimental verification.

Unfortunately, the origin of the 2-$\boldsymbol{k}$ spin structure in the iron oxychalcogenides is not fully understood. Calculations assuming exchange interactions of nearest-neighbor J_1 (via Fe-Fe) and next-nearest neighbor J_2 (via Fe-Se-Fe) and J_2' (via Fe-O-Fe) only yielded collinear-type (π, 0), (π/2, π/2), (π, π) structures.[10] This suggests apparently a necessity to include magnetic anisotropy, imposed presumably by the mixed-anion coordination environment around iron. It is also worth pointing out that the $[Fe_2Ch_2O]$ blocks in all the reported AFe_2Ch_2O are arranged in a staggered manner along the *c* axis. So far, the uniformly stacked version has been exclusively limited to titanium oxypnictides $BaTi_2Pn_2O$ (*Pn* = As, Sb, Bi),[24–27] in which, interestingly, the presence or absence of superconductivity is argued in relation with the stacking sequence.[26] Thus, it would be valuable to explore an iron oxychalcogenide with a uniform stacking of $[Fe_2Ch_2O]$ layers which offers a unique situation to check the influence of the stacking sequence on the magnetic properties.

A high-pressure reaction is an efficient approach for accessing mixed anion compounds as it can obviously avoid undesired evaporation of different anionic species during reaction.[28–31] This technique has been already employed to synthesize a range of iron-based superconductors.[4,5,32] It is rather surprising that there is no report on AM_2Ch_2O and AM_2Pn_2O compounds prepared under high pressure, despite their (apparent) dense structures. Here, we have successfully synthesized $BaFe_2Se_2O$ with a uniform stack of $[Fe_2Se_2O]$ layers using the high pressure strategy (Fig. 1b). Magnetic susceptibility, heat capacity, Mössbauer spectroscopy, and neutron diffraction

measurements revealed that the $BaFe_2Se_2O$ adopts the 2-***k*** magnetic structure as seen in $(Ln_2O_2)Fe_2Se_2O$ (*Ln* = La, Ce, Nd) and $(Sr_2F_2)Fe_2S_2O$ with the staggered sequence.[12,20–22] Together with the DFT calculations, we show that the orthogonal spin structure originates from the magnetic anisotropy of Fe moment imposed by its mixed anion coordination geometry. The presence of strong crystal field splitting of Fe^{2+} is suggested from the recent theoretical work by Whangbo *et al.*.[33]

EXPERIMENTAL DETAILS

A polycrystalline sample of $BaFe_2Se_2O$ was synthesized under high pressure using a cubic anvil press. BaO (99.99%, Aldrich), Fe (99.9%, Kojundo Chemical) and Se (99.9%, Kojundo Chemical) were intimately mixed in stoichiometric ratio in a nitrogen filled glovebox (H_2O, O_2 < 0.1 ppm). The mixture was pressed into a pellet, covered with a Pt foil and loaded in a cubic cell. The sample was heated at 900–1100 °C in applied pressure of 2–6 GPa. The obtained samples were examined by powder X-ray diffraction (XRD) using a D8 ADVANCE diffractometer (Bruker AXS) with Cu-$K\alpha$ radiation. Electrical resistivity was measured by a standard DC four-terminal method using a physical property measurement system (Quantum Design, PPMS). Temperature- and field-dependent magnetizations were measured on a SQUID magnetometer (Quantum Design MPMS). High-field magnetization up to 50 T was measured using a nondestructive pulse magnet by means of a standard induction method at Center for Advanced High Magnetic Field Science, Osaka University. Specific heat was measured by the relaxation method using PPMS. Powder neutron powder diffraction (ND) data were collected between 3 K and 120 K with λ = 2.41 Å using D20 diffractometer at Institut Laue-Langevin (ILL). ^{57}Fe Mössbauer spectra were taken between 4 K and 295 K in transmission geometry using a ^{57}Co/Rh γ-ray source. The source velocity was calibrated by α-Fe. DFT calculations were carried out with VASP[34] using the projector-augmented-wave (PAW) method[35] and the generalized gradient approximations plus on-site repulsion (*U*) method (GGA + *U*) for the exchange and correlation corrections.

RESULTS AND DISCUSSIONS

Shown in Fig. 2 is the XRD pattern of the product obtained at 1000 °C under 5 GPa, which is clearly different from that for $BaFe_2Se_2O$ obtained at ambient pressure (*ap*-$BaFe_2Se_2O$ structure).[36,37] The majority of the observed reflections can be indexed on a primitive tetragonal cell with a = 4.0748(1) Å and c = 7.1501(5) Å, together with unindexed minor impurities. Syntheses under different conditions resulted in substantial increase of byproducts such as Fe_7Se_8 and Fe_3O_4 (Fig. S1 in the Supplemental Material[38]). The cell constants determined are close to those of $BaTi_2As_2O$ (a = 4.047 Å and c = 7.275 Å) consisting of a uniform stacking of $[Ti_2As_2O]$ layers as illustrated in Fig. 1b.[24,27] Indeed, the observed profile resembles the simulated one for $BaFe_2Se_2O$ on the basis of the $BaTi_2As_2O$-type structure with the space group of *P*4/*mmm* (Fig. 2). The density of

the high-pressure form of $BaFe_2Se_2O$ (*hp*-$BaFe_2Se_2O$) is 5.92 g/cm^3, which is higher than 5.14 g/cm^3 in *ap*-$BaFe_2Se_2O$ comprised of $FeOSe_3$ tetrahedra.[36,37]

In order to obtain microscopic information on the magnetic properties, we performed ^{57}Fe Mössbauer experiments. The room-temperature (295 K) spectrum, shown in Fig. 3, consists of three sets of doublets with a spectrum weight of 72:16:12. As will be discussed later, the latter two were assigned as byproducts, a Fe(II)-containing paramagnetic phase (possibly corresponding to $Fe_{1+x}Se$[39]) and a Fe(III)-containing ordered phase. The isomer shift (*IS*) of the main phase is 0.89 mm/s, suggesting a divalent high-spin state (S = 2). In addition, the quadrupole splitting of 1.96 mm/s is close to what has been observed in AFe_2Se_2O (A = Sr_2F_2, Ba_2F_2, and Ln_2O_2) with a staggered stacking of [Fe_2Se_2O] layers (Table S1 in the Supplemental Material). These considerations led us to conclude that *hp*-$BaFe_2Se_2O$ crystalizes in the $BaTi_2As_2O$-type structure, though the presence of unidentified impurities in the XRD profile prevented a precise structural refinement. We note that, prior to this study, $BaTi_2Pn_2O$ was the only example of a compound having the uniform stacking sequence in this structural family.

The localized nature of *hp*-$BaFe_2Se_2O$ is seen from the temperature dependence of the electrical resistivity, with an activation energy of 0.14 eV (Fig. S2 in the Supplemental Material). The temperature dependence of magnetic susceptibility measured at 1 T (0.01 T) is shown in Fig. 4a (Fig. S3 in the Supplemental Material). The susceptibility gradually increases upon cooling, though it deviates from the Curie-Weiss law possibly due to the presence of short-range correlations and/or impurity phases. With further cooling, the susceptibility exhibits an anomaly at around 100–110 K, implying the onset of long-range magenetic order, accompanied by a small deviation between zero-field- and field-cooling processes. The *M*-*H* curve at 2 K (Fig. 4a, inset) shows a small hysteresis loop with a remnant moment of 0.002 μ_B/Fe, suggesting a tiny canting in the AFM state. The specific heat $C(T)$ of *hp*-$BaFe_2Se_2O$ (Fig. 4b) provided a precise estimation of T_N = 106 K, with a clear λ-type anomaly signifying the second-order phase transition. As shown in Fig. 4b, a polynomial fitting was performed to subtract a nonmagnetic contribution from the raw data, and the magnetic entropy release (S_{mag}) associated with the transition was estimated (Fig. 4b, inset) The obtained value of 1.6 Jmol^{-1}K^{-1} is much smaller than 13.4 Jmol^{-1}K^{-1} for S = 2, implying the development of short-range correlations above T_N in the two-dimensional (2D) spin system, as also discussed in $Ln_2O_2Fe_2Se_2O$ and $Na_2Fe_2Se_2O$.[16,17]

Figure 5a is the powder ND patterns at low temperatures, demonstrating magnetic reflections indexed as (h/2, k, l/2) below T_N. The magnetic propagation vector can be determined as $\boldsymbol{k}$ = (1/2 0 1/2) or (0 1/2 1/2). Refinement of the 3 K data with $\boldsymbol{k}$ = (1/2 0 1/2) (shown in Fig. S4 and Table S2 in the Supplemental Material) gave 3.28(5) μ_B for the ordered Fe moment, which is comparable to those of $La_2Fe_2Se_2O$ (3.2 μ_B)[22] and $Sr_2F_2Fe_2S_2O$ (3.3 μ_B)[19]. Upon heating, the (1/2, 1, 1/2) peak gradually decreases and vanishes above 110 K, in agreement with the results of

susceptibility, specific heat, and Mössbauer measurements. The temperature dependence of the ordered Fe moment is shown in Fig. 6. Among possible spin structures, a collinear double stripe structure (Fig. 5c) as found in the $Fe_{1+x}Te$ system[7,40] and the non-collinear 2-***k*** spin structure (Fig. 5d) as found in AFe_2Se_2O (with the staggered stacking sequence)[12,19–22] are likely. As, however, both models result in identical calculated ND patterns, it is not possible to determine the spin structure of our compound from powder ND.

Mössbauer spectroscopy below T_N provides a unique opportunity to distinguish the two spin structures. When the sample is cooled across T_N, the paramagnetic doublet is magnetically split, with the size of the splitting increasing with decreasing temperature. The spectra and detailed information of the impurity phases are provided in Fig. S5 and Table S3 in the Supplemental Material. Figure 3 represents a spectrum at 4 K, which is well assigned, apart from doublets from impurity phases (26%), to a single sextet, providing a clear indication that magnetically the iron environment in *hp*-$BaFe_2Se_2O$ is unique. Additionally, ($S_2 - S_1$) in Fig. 3 is 1.95 mm/s, which is very close to the quadrupole splitting ΔE of 1.96 mm/s in the paramagnetic state at room temperature (Table I). From these facts, we conclude that the spin orientation is parallel to the electric field gradient that is along the Fe-O bond. It is obvious that only the 2-***k*** structure with Fe moments pointing to the neighboring oxide anion (along *a* or *b*) satisfies this requisite. The present result suggests that the 2-***k*** structure is fairly robust against the choice of stacking sequence.

A strong uniaxial spin anisotropy is inferred from the orthogonal spin arrangement in *hp*-$BaFe_2Se_2O$ and related oxyselenides. For extended transition-metal oxides/halides, such a uniaxial anisotropy has been observed in systems with the d^6 electronic configuration, such as $CsCoCl_3$,[41] $Ca_3Co_2O_6$,[42] and $BaFe_2(PO_4)_2$,[43] where a nearly cubic $Co^{3+}L_6$ and $Fe^{2+}L_6$ octahedral environment (L = ligand) gives rise to a partial orbital degree of freedom and resultant spin-orbit coupling (SOC). This mechanism, however, cannot be applied to our and related compounds containing highly distorted FeO_2Se_4 octahedron. An alternate mechanism for the strong uniaxial anisotropy is found in single molecular magnets including $Fe^{2+}[C(SiMe_3)_3]_2$,[44] $Co^{2+}[N(H)Ar']_2$ (Ar' = C_6H_3-2,6(C_6H_2-2,4,6-Pr^i_3)$_2$),[45] and $[Ni^+(6\text{-Mes})_2]Br$ (6-Mes = 1,3-bis(2,4,6-trimethylphenyl)-3,4,5,6-tetrahydropyrimidin-2-ylidende).[46] These molecular complexes adopt a linear-coordination geometry around the *d* metal centre, which lifts the degeneracy of *d* orbitals within a narrow energy range and generates a non-negligible contribution of SOC as a perturbation to the inherent spin orientation.[47,48] We speculate that a similar situation occurs in our and related systems. Here, the Fe-O distance in the *trans*-FeO_2Se_4 octahedron is much shorter than the Fe-Se one (e.g. $d_{Fe\text{-}O}$ = 2.039 Å, $d_{Fe\text{-}Se}$ = 2.722 Å in $La_2O_2Fe_2Se_2O$)[8]. In addition, the oxygen atom has larger electronegativity and smaller polarizability relative to selenium. These facts suggest that the oxide ion is a much stronger ligand for Fe(II) than the selenide ion, and could be regarded as a quasi-linear coordination geometry. The *M*-*H* measurement at 4.2 K shows a linear

field dependence up to H = 50 T (Fig. S6 in the Supplemental Material), supporting the fairly strong uniaxial anisotropy derived from the heteroleptic Fe coordination.

Recently, it has been theoretically shown that the spin orientation is predictable by analyzing the angular properties of the metal *d* orbitals present in the HOMO and LUMO.[33] Figure 7 represents how the *d*-orbital degeneracy is lifted in the *trans*-Fe(II)O_2Se_4 environment, where for simplicity the local *x*/*y*- and *z*-axes are set along the Fe-Se and Fe-O bonds, respectively, and the Se-Fe-Se angle (~97°) is approximated as 90°. One can see that the 6th down-spin fills the *xy* orbital (magnetic HOMO), whereas there are two choices regarding magnetic LUMO, the (nearly) degenerate *yz*/*zx* levels (case 1) or the x^2–y^2 level (case 2), depending on the magnitude of the crystal field splitting energy. For case 1, the HOMO-LUMO interaction between the filled $xy\downarrow$ and the empty $yz/zx\downarrow$ states ($|\Delta L_z| = 1$) gives the preferred spin direction of $\perp z$, i.e., parallel to the $FeSe_4$ plane, which disagrees with the experimental result. On the other hand, for case 2 the preferred spin direction of //z (i.e., parallel to the Fe-O bond) is derived from the HOMO-LUMO interaction between the filled $xy\downarrow$ and the empty $x^2-y^2\downarrow$ ($|\Delta L_z| = 0$). This agrees with the experimental observation and supports our view that the local Fe environment is regarded as quasi-linear.

As already addressed, theoretical calculations on $A$$Fe_2$$Ch_2$O have been so far limited to the isotropic model that only yields collinear spin structures.[10] Thus, spin-orbit interaction was included in our self-consistent calculation for a (simpler) 2-***k*** spin structure with a magnetic unit cell that is related to the crystal one by 2 × 2 × 1. We used an on-site repulsion of U = 3 eV and a plane-wave cutoff energy of 500 eV. It is found that the Fe moment vanished without inclusion of SOC, whereas inclusion of SOC provided an unquenched orbital momentum of 0.1 μ_B/Fe, along with the spin component of 3.2 μ_B/Fe, which is consistent with the experimental result and reasonable for high-spin d^6 system. The density of states (DOS) in Fig. 8 revealed an energy gap of ~0.5 eV at the Fermi level, in accordance with the insulating nature of this material. We also calculated a collinear double stripe structure (Fig. 5c) with a 2 × 1 × 1 magnetic cell assuming U = 3 eV and found that this model is less stable by 0.017 eV/Fe.

CONCLUSION

The high-pressure phase of $BaFe_2Se_2O$ with a uniform stacking of [Fe_2Se_2O] layers was obtained. *hp*-$BaFe_2Se_2O$ undergoes a long-range magnetic ordering below 106 K with the 2-***k*** spin structure, as observed in the related layered iron oxychalcogenides with a staggered stacking sequence, revealing that the 2-***k*** spin structure is fairly stable for compounds with [Fe_2Ch_2O] layers regardless of the stacking manner. The uniaxial anisotropy of Fe^{2+} moment implies the presence of SOC derived from the mixed anionic *trans*-FeO_2Se_4 (FeO_2S_4) octahedron. The analysis of $|\Delta L_z|$ associated with the HOMO-LUMO interactions suggests a considerable stabilization of the x^2–y^2 orbital. We suggest that this local geometry is effectively considered as *quasi*-linear owing to the

marked difference of the length to the metal center, electronegativity and polarizability between O and Se(S). The linear coordination can be often seen in molecular complexes, but the central metals are isolated or only weakly interacting because they are separated by molecular ligands. Creating linear coordination by using different mono-anionic anions has a crucial advantage in designing extended lattices (square lattice etc.) that cause novel phenomena based on strongly correlated spins and electrons, such as unusual spin structures as found in the present study.

ACKNOWLEDGMENT

We thank Y. Ajiro and T. Fujihara for helpful discussions. This work was mostly supported by CREST project and Grant-in-Aid for Challenging Exploratory Research (26620044) and partly by Grant-in-Aid for Scientific Research on Innovative Areas (JP16H06439, JP16H06440). The high-field magnetization experiment was carried out at the Center for Advanced High Magnetic Field Science in Osaka University under the Visiting Researcher's Program of the Institute for Solid State Physics, the University of Tokyo. F.T. was supported by JSPS for Young Scientists.

REFERENCES

[1] Y. Kamihara, T. Watanabe, M. Hirano, and H. Hosono, J. Am. Chem. Soc. **130**, 3296 (2008).

[2] J. Paglione and R. L. Greene, Nat. Phys. **6**, 645 (2010).

[3] P. Dai, J. Hu, and E. Dagotto, Nat. Phys. **8**, 709 (2012).

[4] S. Iimura, S. Matsuishi, H. Sato, T. Hanna, Y. Muraba, S. W. Kim, J. E. Kim, M. Takata, and H. Hosono, Nat. Commun. **3**, 943 (2012).

[5] M. Hiraishi, S. Iimura, K. M. Kojima, J. Yamaura, H. Hiraka, K. Ikeda, P. Miao, Y. Ishikawa, S. Torii, M. Miyazaki, I. Yamauchi, A. Koda, K. Ishii, M. Yoshida, J. Mizuki, R. Kadono, R. Kumai, T. Kamiyama, T. Otomo, Y. Murakami, S. Matsuishi, and H. Hosono, Nat. Phys. **10**, 300 (2014).

[6] S. Li, C. De La Cruz, Q. Huang, Y. Chen, J. W. Lynn, J. Hu, Y. L. Huang, F. C. Hsu, K. W. Yeh, M. K. Wu, and P. Dai, Phys. Rev. B **79**, 054503 (2009).

[7] W. Bao, Y. Qiu, Q. Huang, M. A. Green, P. Zajdel, M. R. Fitzsimmons, M. Zhernenkov, S. Chang, M. Fang, B. Qian, E. K. Vehstedt, J. Yang, H. M. Pham, L. Spinu, and Z. Q. Mao, Phys. Rev. Lett. **102**, 247001 (2009).

[8] J. M. Mayer, L. F. Schneemeyer, T. Siegrist, J. V Waszczak, and B. Van Dover, Angew. Chem. Int. Ed. Engl. **31**, 1645 (1992).

[9] H. Kabbour, E. Janod, B. Corraze, M. Danot, C. Lee, M.-H. Whangbo, and L. Cario, J. Am. Chem. Soc. **130**, 8261 (2008).

[10] J. X. Zhu, R. Yu, H. Wang, L. L. Zhao, M. D. Jones, J. Dai, E. Abrahams, E. Morosan, M. Fang, and Q. Si, Phys. Rev. Lett. **104**, 216405 (2010).

[11] D. G. Free and J. S. O. Evans, Phys. Rev. B **81**, 214433 (2010).

[12] Y. Fuwa, M. Wakeshima, and Y. Hinatsu, J. Phys. Condens. Matter **22**, 346003 (2010).

[13] C. Wang, M. Q. Tan, C. M. Feng, Z. F. Ma, S. Jiang, Z. A. Xu, G. H. Cao, K. Matsubayashi, and Y. Uwatoko, J. Am. Chem. Soc. **132**, 7069 (2010).

[14] Y. Fuwa, T. Endo, M. Wakeshima, Y. Hinatsu, and K. Ohyama, J. Am. Chem. Soc. **132**, 18020 (2010).

[15] D. G. Free, N. D. Withers, P. J. Hickey, and J. S. O. Evans, Chem. Mater. **23**, 1625 (2011).

[16] N. Ni, E. Climent-Pascual, S. Jia, Q. Huang, and R. J. Cava, Phys. Rev. B **82**, 214419 (2010).

[17] J. B. He, D. M. Wang, H. L. Shi, H. X. Yang, J. Q. Li, and G. F. Chen, Phys. Rev. B **84**, 205212 (2011).

[18] N. Ni, S. Jia, Q. Huang, E. Climent-Pascual, and R. J. Cava, Phys. Rev. B **83**, 224403 (2011).

[19] L. L. Zhao, S. Wu, J. K. Wang, J. P. Hodges, C. Broholm, and E. Morosan, Phys. Rev. B **87**, 020406 (2013).

[20] E. E. McCabe, C. Stock, E. E. Rodriguez, A. S. Wills, J. W. Taylor, and J. S. O. Evans, Phys. Rev. B **89**, 100402 (2014).

[21] E. E. McCabe, A. S. Wills, L. Chapon, P. Manuel, and J. S. O. Evans, Phys. Rev. B **90**, 165111 (2014).

[22] M. Günther, S. Kamusella, R. Sarkar, T. Goltz, H. Luetkens, G. Pascua, S.-H. Do, K.-Y. Choi, H. D. Zhou, C. G. F. Blum, S. Wurmehl, B. Büchner, and H.-H. Klauss, Phys. Rev. B **90**, 184408 (2014).

[23] G. Giovannetti, C. Ortix, M. Marsman, M. Capone, J. van den Brink, and J. Lorenzana, Nat. Commun. **2**, 398 (2011).

[24] X. F. Wang, Y. J. Yan, J. J. Ying, Q. J. Li, M. Zhang, N. Xu, and X. H. Chen, J. Phys. Condens. Matter **22**, 075702 (2010).

[25] T. Yajima, K. Nakano, F. Takeiri, T. Ono, Y. Hosokoshi, Y. Matsushita, J. Hester, Y. Kobayashi, and H. Kageyama, J. Phys. Soc. Jpn. **81**, 103706 (2012).

[26] T. Yajima, K. Nakano, F. Takeiri, J. Hester, T. Yamamoto, Y. Kobayashi, N. Tsuji, J. Kim, A. Fujiwara, and H. Kageyama, J. Phys. Soc. Jpn. **82**, 013703 (2013).

[27] T. Yajima, K. Nakano, F. Takeiri, Y. Nozaki, Y. Kobayashi, and H. Kageyama, J. Phys. Soc. Jpn. **82**, 033705 (2013).

[28] B. L. Chamberland, Mater. Res. Bull. **6**, 311 (1971).

[29] Z. Hiroi, N. Kobayashi, and M. Takano, Nature **371**, 139 (1994).

[30] M. Yang, J. A. Rodgers, L. C. Middler, J. Oró-Solé, A. B. Jorge, A. Fuertes, and J. P. Attfield, Inorg. Chem. **48**, 11498 (2009).

[31] C. Tassel, Y. Goto, Y. Kuno, J. Hester, M. Green, Y. Kobayashi, and H. Kageyama, Angew. Chem. Int. Ed. **53**, 10377 (2014).

[32] P. M. Shirage, K. Kihou, C. H. Lee, H. Kito, H. Eisaki, and A. Iyo, J. Am. Chem. Soc. **133**, 9630

(2011).

[33] M. H. Whangbo, E. E. Gordon, H. Xiang, H. J. Koo, and C. Lee, Acc. Chem. Res. **48**, 3080 (2015).

[34] G. Kresse and J. Hafner, Phys. Rev. B **47**, 558(R) (1993); G. Kresse and J. Furthemüller, Phys. Rev. B **54**, 11169 (1996).

[35] D. Hobbs, G. Kresse, and J. Hafner, Phys. Rev. B **62**, 11556 (2000).

[36] F. Han, X. Wan, B. Shen, and H. H. Wen, Phys. Rev. B **86**, 014411 (2012).

[37] H. Lei, H. Ryu, V. Ivanovski, J. B. Warren, A. I. Frenkel, B. Cekic, W.-G. Yin, and C. Petrovic, Phys. Rev. B **86**, 195133 (2012).

[38] See Supplemental Material at [*URL will be inserted by publisher*] for the XRD patterns under several reaction conditions, electrical resistivity, susceptibility at small magnetic field, temperature variaties of Mössbauer spectra, refinement of powder ND at 3 K, magnetization up to 50 T at 4.2 K, and Mössbauer parameters with those of the related oxyselenides.

[39] T. M. McQueen, Q. Huang, V. Ksenofontov, C. Felser, Q. Xu, H. Zandbergen, Y. S. Hor, J. Allred, A. J. Williams, D. Qu, J. Checkelsky, N. P. Ong, and R. J. Cava, Phys. Rev. B **79**, 014522 (2009).

[40] E. E. Rodriguez, C. Stock, P. Zajdel, K. L. Krycka, C. F. Majkrzak, P. Zavalij, and M. A. Green, Phys. Rev. B **84**, 064403 (2011).

[41] M. Mekata and K. Adachi, J. Phys. Soc. Jpn. **44**, 806 (1978).

[42] H. Kageyama, K. Yoshimura, K. Kosuge, M. Azuma, M. Takano, H. Mitamura, T. Goto, J. Phys. Soc. Jpn. **66**, 3996 (1997).

[43] H. Kabbour, R. David, A. Pautrat, H. J. Koo, M. H. Whangbo, G. André, and O. Mentré, Angew. Chem. Int. Ed. **51**, 11745 (2012).

[44] W. M. Reiff, A. M. LaPointe, and E. H. Witten, J. Am. Chem. Soc. **126**, 10206 (2004).

[45] A. M. Bryan, W. A. Merrill, W. M. Reiff, J. C. Fettinger, and P. P. Power, Inorg. Chem. **51**, 3366 (2012).

[46] R. C. Poulten, M. J. Page, A. G. Algarra, J. J. Le Roy, I. López, E. Carter, A. Llobet, S. A. Macgregor, M. F. Mahon, D. M. Murphy, M. Murugesu, and M. K. Whittlesey, J. Am. Chem. Soc. **135**, 13640 (2013).

[47] P. P. Power, Chem. Rev. **112**, 3482 (2012).

[48] J. M. Zadrozny, D. J. Xiao, M. Atanasov, G. J. Long, F. Grandjean, F. Neese, and J. R. Long, Nat. Chem. **5**, 577 (2013).

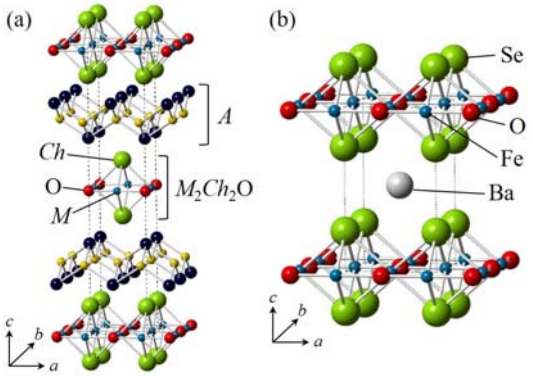

FIG. 1. (a) AM_2Ch_2O (A^{2+} = $(Ln_2O_2)^{2+}$ (Ln = lanthanides), $(Sr_2F_2)^{2+}$, $(Ba_2F_2)^{2+}$, $(Na_2)^{2+}$; M = Mn, Fe, Co; Ch = S, Se) with a staggered stacking of [M_2Ch_2O] layers.[8–19] (b) *hp*-$BaFe_2Se_2O$ with a uniform stacking of [Fe_2Se_2O] layers.

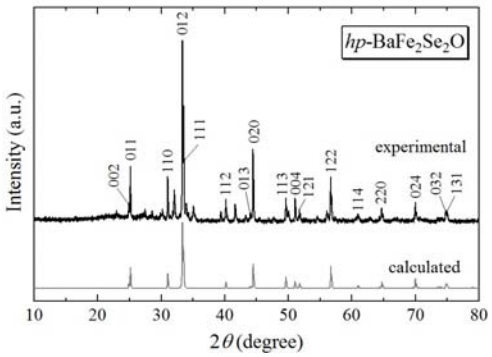

FIG. 2. The experimental (upper) and calculated (lower) XRD pattern for *hp*-$BaFe_2Se_2O$ with the $BaTi_2As_2O$-type structure.

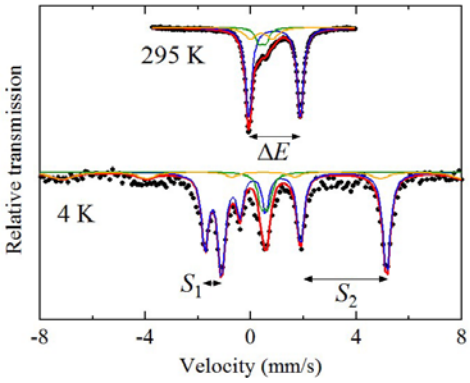

FIG. 3. Mössbauer spectra for *hp*-$BaFe_2Se_2O$ at 295 K and 4 K. For each temperature, the blue line represents the subspectrum for *hp*-$BaFe_2Se_2O$, while the green and yellow lines correspond to byproducts, possibly $Fe_{1+x}Se$ and an unknown phase with Fe^{3+}, respectively. The red line represents the total fit.

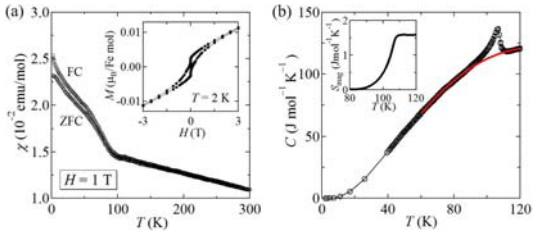

FIG. 4. (a) Temperature dependence of the magnetic susceptibility of *hp*-$BaFe_2Se_2O$ at 1 T measured in FC and ZFC processes. The inset represents the $M(H)$ curve at 2 K. (b) Specific heat for *hp*-$BaFe_2Se_2O$ in zero field. The red curve represents a polynomial fitting for 60–120 K. The inset represents the estimated magnetic contribution to the entropy.

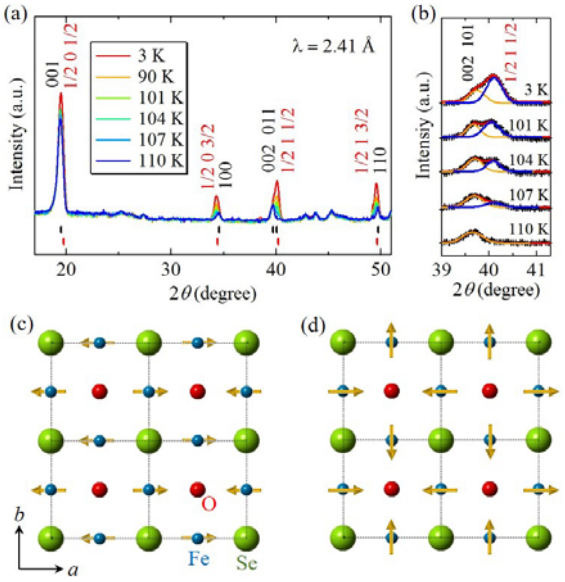

FIG. 5. (a) Powder ND patterns of *hp*-$BaFe_2Se_2O$ at low temperatures. The ticks indicate the calculated positions of nuclear (upper) and magnetic (lower) reflections. (b) The enlarged plot around the (1/2, 1, 1/2) reflection. We fitted the profiles using two Gaussians. The blue and yellow lines represent the magnetic and nuclear reflections, respectively, and the red line is the total fit. The lower panels show magnetic structures compatible with (*h*/2, *k*, *l*/2) reflections: (c) a double stripe structure and (d) a 2-***k*** structure.

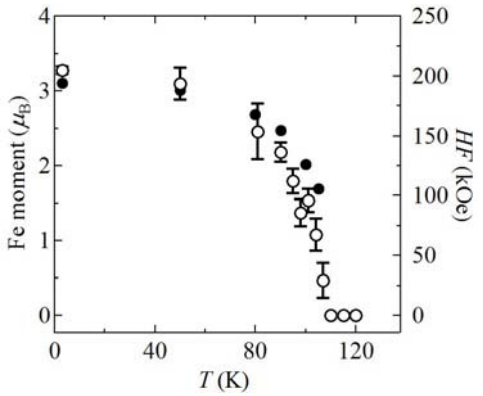

FIG. 6. Temperature dependence of the magnetic moment obtained from powder ND (open) and hyperfine field (*HF*) obtained from Mössbauer (closed) for *hp*-$BaFe_2Se_2O$. The magnetic moment shown here is obtained by normalizing the square root of the neutron scattering intensity of (1/2, 1, 1/2) to the refined value of 3.28(5) μ_B at 3K.

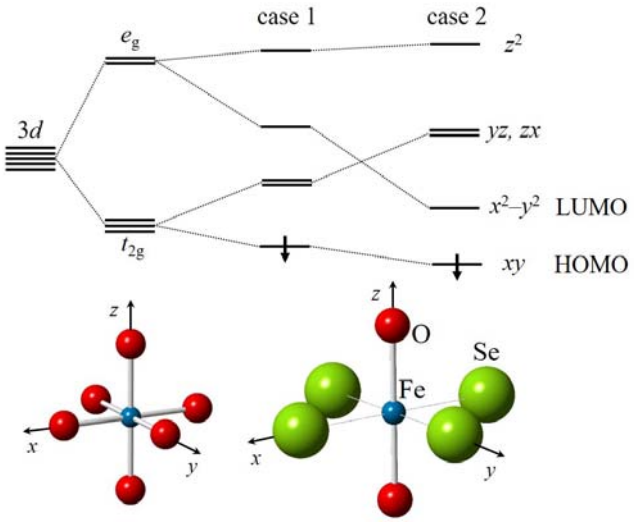

FIG. 7. The expected scheme of the crystal field splitting of Fe 3*d* orbitals in the *trans*-FeO_2Se_4 octahedron, where only the 6th down-spin is shown for high-spin ($S = 2$) state.

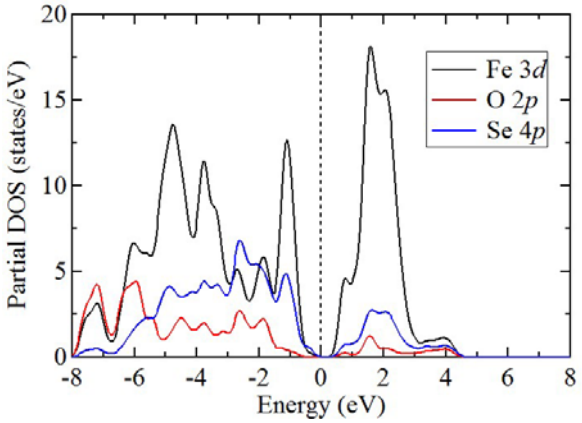

FIG. 8. The partial DOS for *hp*-$BaFe_2Se_2O$ calculated by using the 2-***k*** magnetic structure with on-site repulsion of $U = 3$ eV.

TABLE I. Mössbauer parameters for *hp*-$BaFe_2Se_2O$.

T	*IS* (mm/s)	*HF* (kOe)	*QS* (mm/s)	*FWHM* (mm/s)
295 K	0.89	0	1.96	0.28
4 K	1.04	194	1.95	0.30

IS, *HF*, *QS*, and *FWHM* represent isomer shift, hyperfine field, quadrupole splitting, and full width at half maximum, respectively. The *QS* at 4 K is equivalent to ($S_2 - S_1$) in Fig. 3.